

Effects of Pulsating Flow on Mass Flow Balance and Surge Margin in Parallel Turbocharged Engines

Andreas Thomasson¹ Lars Eriksson¹

¹Department of Electrical Engineering, Linköping University, Sweden, {andreast, larer}@isy.liu.se

Abstract

The paper extends a mean value model of a parallel turbocharged internal combustion engine with a crank angle resolved cylinder model. The result is a 0D engine model that includes the pulsating flow from the intake and exhaust valves. The model captures variations in turbo speed and pressure, and therefore variations in the compressor operating point, during an engine cycle. The model is used to study the effect of the pulsating flow on mass flow balance and surge margin in parallel turbocharged engines, where two compressors are connected to a common intake manifold. This configuration is harder to control compared to single turbocharged systems, since the compressors interact and can work against each other, resulting in co-surge. Even with equal average compressor speed and flow, the engine pulsations introduce an oscillation in the turbo speeds and mass flow over the engine cycle. This simulation study use the developed model to investigate how the engine pulsations affect the in cycle variation in compressor operating point and the sensitivity to co-surge. It also shows how a short circuit pipe between the two exhaust manifolds could increase surge margin at the expense of less available turbine energy.

Keywords: Engine modeling, Engine simulation, Compressor surge, Turbocharging

1 Introduction

Turbocharging is now days a common way to increase power density and reduce fuel consumption of internal combustion engines Emmenthal et al. (1979); Guzzella et al. (2000). To make further improvement and meet increasing demands, more advanced turbocharging concepts have been developed over the years (Petitjean et al., 2004; Galindo et al., 2009), that are now being put into production on a larger scale. One such concept that is used for V-type engines is to have two smaller, parallel turbochargers, where each turbine is feed by one of the two cylinder banks. This enables the turbines to be placed closer to the exhaust ports, reducing the size of the exhaust manifold and results in better utilization of the energy in the exhaust pulses Watson and Janota (1982).

Usually the two compressors are then connected to a common intake manifold, which is the configuration studied in this paper. This ensures that the intake pressure is equal for all cylinders, but introduces another balancing problem. If the two compressors does not produce equal flow, one compressor will be operating closer to the surge line than the other, and possibly go into surge even if the average operating point would be stable. When the surging compressor recovers it can then push the other compressor into surge, resulting in a mass flow oscillation between the two compressors that alternately go into surge. This phenomena has been investigated in Thomasson and Eriksson (2014), that also shows how the main behavior of the co-surge oscillation can be captured by a Mean Value Engine Model (MVEM), without considering in-cycle variations.

Due to the pulsations from the intake and exhaust valves, turbo speed and flow variations will occur during an engine cycle, even if the two compressors operates with equal average flow. To be able to capture these phenomena, and see how they can effect surge sensitivity, the MVEM is not sufficient. However the extension to a crank angle resolved 0D model requires only the cylinder model to be replaced. With that extension and the assumption that the MVEM submodels can be used in a quasi stationary pulsating flow, the in-cycle variations can be modeled.

1.1 Contributions

The paper integrates a crank angel resolved cylinder model in an existing MVEM. The resulting zero dimensional model is used to study the effect of cylinder pulsations on mass flow balance in parallel turbocharged V-engines. The effect of intake pulsations, exhaust pulsation and cylinder firing order is investigated separately, where the later is shown to have a very large impact on the in-cycle turbo speed variations for V8-engines. This is an important aspect when designing parallel turbocharge engines, as a too large compressor choice could otherwise make the system very sensitive to surge. The paper also shows how a short circuit pipe between the two exhaust manifolds could increase the surge margin, with the downside that a part of the available energy in the exhaust pulses are lost.

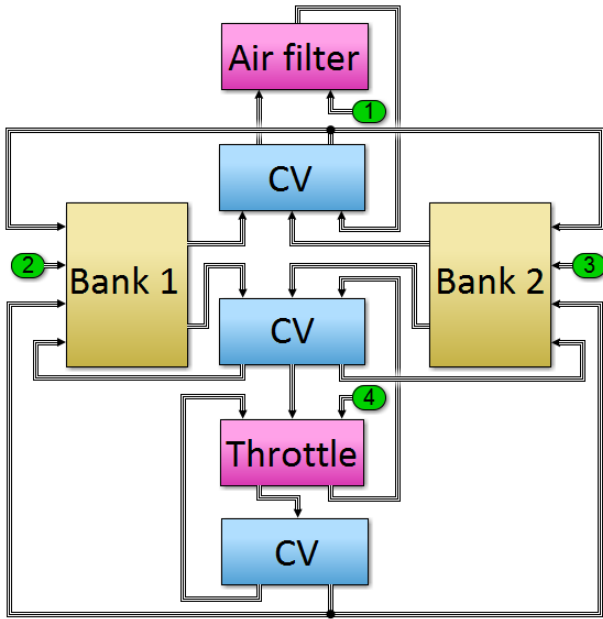


Figure 1. An overview of the simulink MVEM for the parallel turbocharged engine. Magenta colored blocks are restrictions (Air filter, Throttle), blue are control volumes (CV) and yellow blocks are collections of other blocks (Bank 1,2), in this case all doubled blocks: compressor, compressor CV, intercooler, cylinder bank, exhaust manifold CV, turbine, turbine CV and exhaust restriction.

2 Engine Model

A common approach in engine control is to work with Mean Value Engine Models (MVEM). These models are zero dimensional and does not resolve variations that occur during a cycle, which are instead averaged, resulting in very fast simulation models. These models started to develop in the late 80's and early 90's (Hendricks, 1989; Hendricks and Sorenson, 1990; Jensen et al., 1991), and soon started to be used for engine control, see for example Guzzella and Amstutz (1998). The starting point for the model in this investigation is a component based MVEM presented in Eriksson (2007), that has been arranged in a parallel turbocharged engine configuration outlined in Thomasson and Eriksson (2011, 2014). An overview of the model can be seen in Fig. 1.

2.1 Compressor Model

To capture the surge behavior in the compressor the Moore-Greitzer model is used Greitzer (1976, 1981); Hansen et al. (1981). It incorporates a state equation for the mass flow in the compressor

$$\frac{dW_c}{dt} = \frac{\pi D^2}{4L} (\hat{p}_{ac} - p_{ac}) \quad (1)$$

where \hat{p}_{ac} is the pressure build up after the compressor that is given by the compressor map as function of turbo speed and current compressor mass flow. To model the compressor speed lines and extrapolate the compressor

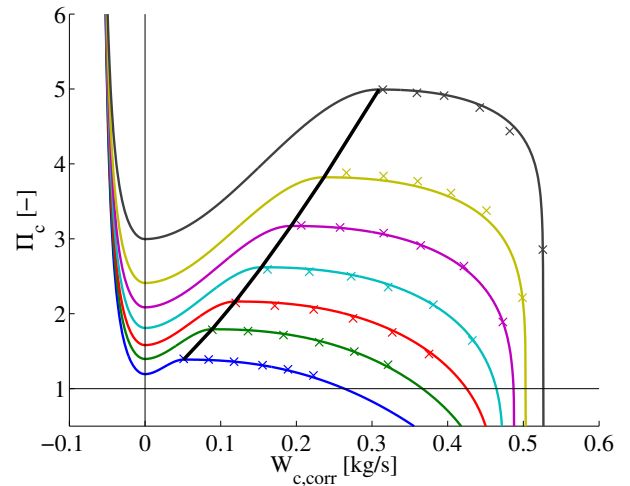


Figure 2. Model of the compressor speed lines together with the measured compressor map (crosses). The model is able to accurately capture the measured compressor map, offer interpolation in the map and extrapolation to the surge and choke region.

map to the surge region, the model presented in Leufvén and Eriksson (2013) is used, which has been shown to model compressor surge with good accuracy together with mean value engine models. The model fit to the measured compressor map and how the speed lines are extrapolated to the surge region are shown in Fig. 2.

2.1.1 Turbo shaft torque balance

The torque balance of the compressors are modeled with Newtons second law of motion for rotating systems, using the power balance between the turbine and the compressor with a viscous friction loss:

$$J_{tc} \frac{\omega_{tc}}{dt} = \frac{P_t}{\omega_{tc}} - \frac{P_c}{\omega_{tc}} - k_{fric} \omega_{tc} \quad (2)$$

The parameters are the compressor inertia, J_{tc} , the turbine power P_t , the compressor power P_c , the turbo speed, ω_{tc} , and the friction coefficient k_{fric} .

2.2 Model Extension to Valve Pulsations

To include the effect of pulsations from the intake and exhaust valves, the MVEM concept has to be abandoned to some extent. However since all components in the model are zero dimensional with filling and emptying dynamics, a first approach is to exchange only the engine block with a crank angle resolved model. The assumption that is made is that the submodels works approximately correct also under quasi-stationary conditions, with cyclic variations around the same mean value as in the MVEM. The new engine model needs to include restrictions to represent the intake and exhaust valves and variable size control volumes to represent the cylinders. Furthermore a model for the heat release from the combustion and heat losses in the cylinder have to be included.

2.2.1 Intake and Exhaust Valves

The intake and exhaust valves are modeled as compressible flow restrictions, with a crank angle dependent effective area. The valve flow area in this model is approximated with the lift times the circumference of the valve,

$$W = \frac{p_{us}}{\sqrt{RT_{us}}} A_{eff} \Psi(\Pi) \quad (3a)$$

$$A_{eff} = C_d L_v(\theta) D_v \pi \quad (3b)$$

where W is the mass flow, A_{eff} is the effective area, D_v is the valve diameter, L_v is the valve lift that depend on the valve profile and the crank angle, θ , and $\Pi = p_{ds}/p_{us}$ is the pressure ratio. The Ψ function is given by

$$\Psi(\Pi) = \begin{cases} \Pi^{1/\gamma} \left\{ \frac{2\gamma}{\gamma-1} \left[1 - \Pi^{\frac{\gamma-1}{\gamma}} \right] \right\}^{1/2} & \text{if } \Pi \geq \Pi_{crit} \\ \gamma^{1/2} \left(\frac{2\gamma}{\gamma+1} \right)^{\frac{\gamma+1}{2(\gamma-1)}} & \text{if } \Pi < \Pi_{crit} \end{cases} \quad (4)$$

where γ is the ratio of specific heats for the gas upstream of the valve. In general the flow area is a more complicated function of the valve and valve seat geometry, see for example Heywood (1988), but this is a good first approximation and enough to get reasonable flow pulsations in the intake and exhaust manifolds.

2.2.2 Cylinder Volume

The cylinder volume is treated a single-zone open system with four states, air mass, m_a , fuel mass, m_f , burned gas mass, m_b , and temperature, T . The mass balance for normal flow direction, from intake to cylinder and from cylinder to exhaust, is given by

$$\dot{m}_a = W_{ip}(1 - x_{b,im}) - W_{ep}x_a - W_{br}(A/F)_s \quad (5a)$$

$$\dot{m}_f = W_f - W_{br} \quad (5b)$$

$$\dot{m}_b = W_{ip}x_{b,im} - W_{ep}x_b + W_{br}(1 + (A/F)_s) \quad (5c)$$

where W_{ip} , W_{ep} and W_f is the intake, exhaust and fuel flow respectively, W_{br} is the fuel burn ratio and $(A/F)_s$ is the stoichiometric air/fuel ratio. The mass fractions are

$$x_a = \frac{m_a}{m_{tot}} \quad x_b = \frac{m_b}{m_{tot}} \quad x_f = \frac{m_f}{m_{tot}} \quad (6)$$

$$m_{tot} = m_a + m_b + m_f$$

where m_{tot} is the total cylinder mass in the cylinder and $x_{b,im}$ in (5) refer to the burned gas fraction in the intake manifold.

The equation for the temperature differential can be derived from the first law of thermodynamics. Under the assumption that the internal energy is only a function of temperature and that the gas mixture can be treated as an ideal gas the result is

$$\dot{T} = -\frac{(\gamma-1)RT}{V} + \frac{1}{c_v(T)m_{tot}} \times \dots \left(\dot{Q}_{hr} - \dot{Q}_{ht} - \sum_i (h_i(T_i) - u_i(T)) W_i \right) \quad (7)$$

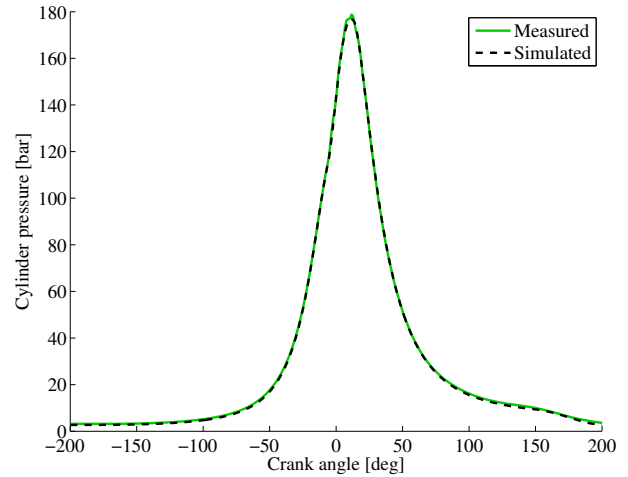


Figure 3. Measured and simulated cylinder pressure trace at 1400 rpm. The model can accurately capture the measured cylinder pressure trace.

where the subscript i indicate the i :th flow component. Three mass flows can occur in this model, gas mixture flowing through the intake and exhaust valves, and fuel flow to the cylinder volume.

2.2.3 Heat Release

To get the fuel burn ratio, a model presented in Chmela and Orthaber (1999) has been used for the heat release rate, \dot{Q}_{hr} . It is based on mixing controlled combustion and in addition to the instantaneous fuel mass in the cylinder considers both injection rate as well as the kinetic energy in the fuel spray. The fuel burn ratio are then calculated from the heat release rate using

$$\dot{Q}_{hr} = W_{br} q_{LHV} \quad (8)$$

where q_{LHV} is the lower heating value of the fuel.

2.2.4 Heat Transfer

The final component of the cylinder model is the heat transfer from the volume to the cylinder walls and piston. This is obtained by Newton's law of cooling

$$\dot{Q}_{ht} = h_c A (T - T_w) \quad (9)$$

where Woschni's heat transfer correlation (Woschni, 1967) is used for the instantaneous heat transfer coefficient, h_c .

2.3 Model Validation

The crank angle resolved cylinder model is validated by comparing the simulated cylinder pressure with measurements. A simulated and measured cylinder pressure trace at 1400 rpm can be seen in Fig. 3. The model is able to capture the cylinder pressure trace very well, and the resulting torque is within 2% of the measured value at this operating point. This accuracy is considered more than enough to get reasonably accurate exhaust pulsations which is the main purpose to introduce this submodel in this study.

3 Simulation Study

In this section the engine model outlined above is used to analyze how engine pulsations affect the mass flow balance in parallel turbocharged engines.

A steady state simulation of a parallel turbocharged V8 engine at 1400 rpm is shown in Fig. 4. The variations in intake side pressures are small, less than 1 %, but the instantaneous mass flow through each compressor varies a lot although the sum is almost constant. It should be emphasized that this is the modeled instantaneous mass flow based on the turbo speed, pressure ratio over the compressor and the compressor map, slightly low pass filtered by the gas inertia included in the Moore-Greitzer model. The shape of the mass flow oscillation is almost identical to the oscillation in compressor speed, indicating that the turbo speed variations is the main reason for mass flow variations. The amplitude of the turbo speed oscillation is around $\pm 1.7\%$ of the average turbo speed. This is larger than for a single turbocharged four cylinder engine, see for example Westin (2005) where a $\pm 0.4\%$ oscillation for a car sized turbo is shown. The main reason for this is the firing order, since the largest shift in turbo speed occurs when two cylinders fire in sequence on one bank. This effect is investigated further in Section 3.3.

3.1 Effect of intake pulsations

As the simulation shown in Fig. 4 shows, the intake side pulses are very small compared the exhaust, and could therefore be expected to have only a minor influence compared to other effects. The size of pulsations are largely influenced by the volumes on the intake side, and to confirm this hypothesis, the model was simulated with a significantly larger volumes on the intake side. Apart from low pass filtering the pressures on the intake side this has only a marginal effect on the turbo speed and instantaneous mass flow through the compressors. The result became almost identical in steady state compared to Fig. 4 and is not shown here. It is concluded that the pressure pulsations on the intake side has very little effect on the mass flow balance.

3.2 Effect of exhaust pulsations

To utilize as much as possible of the exhaust energy in the turbine, the exhaust manifold of turbocharged engines are usually small. This increases the available energy to the turbine but also introduces large cyclic variations in exhaust pressure. To see how large impact the exhaust pulsations have on the parallel turbocharged engine, the model is simulated with a ten times larger exhaust manifold. This low pass filters the pressure pulsations, and reduces the turbo speed oscillation significantly to approximately $\pm 0.6\%$, see Fig. 5. Another way to test the effect of pulsating turbine power is to increase the inertia of the turbocharger. This slows down the turbo dynamics, low pass filtering the speed oscillation without effecting the size of the exhaust

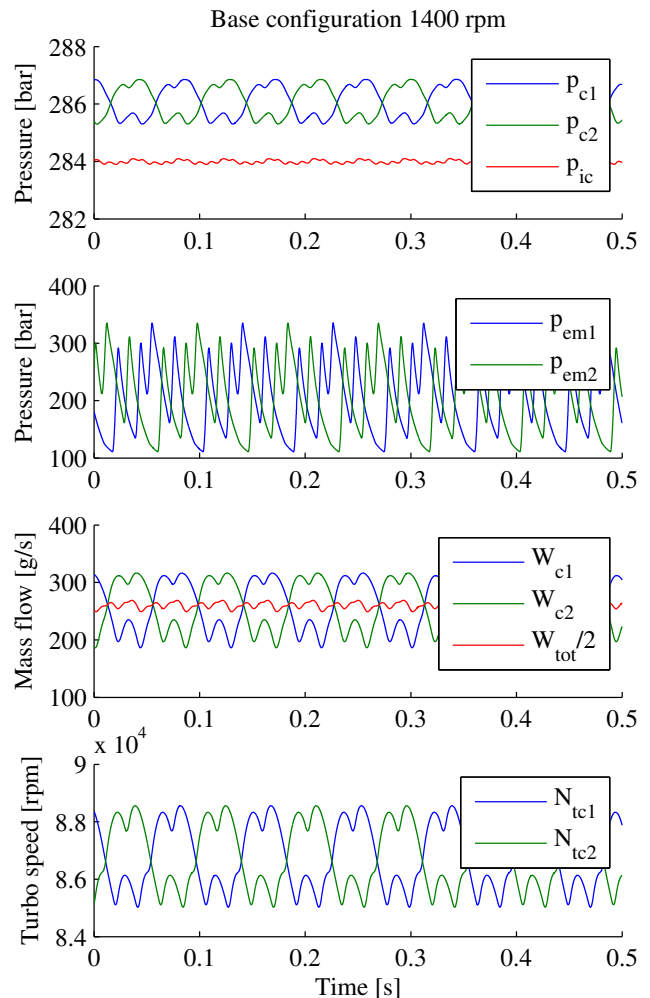


Figure 4. Simulation in a steady state operating point at 1400 rpm. The subscripts are c for compressor, ic for intercooler, em for exhaust manifold and tc for turbocharger. The intake pressure oscillations are small, however the instantaneous mass flow through the compressors pulsates shows large variations over the cycle.

pulses. Doubling the inertia has a similar effect on the turbo speed oscillation as the increased exhaust manifold simulation. It is clear that the major part of the oscillation in the instantaneous mass flow is due to the variations in turbo speed oscillation as a result of the exhaust pulses.

3.3 Effect of the firing order for V8 engines

As discussed earlier, the largest shift in speed between the turbochargers is when two cylinders fire sequentially on one bank. In V8 engines this is used to achieve second order balance, and therefore can not be changed in practice. However, the size of the effect is interesting to study in simulation to understand the limitation, and possibly find solutions. A simulation in the same operating point as previously, but with altered ignition order so that the two banks alternately fires one cylinder during the whole cycle, is shown in Fig. 6. With this firing order, the turbo speed variations are reduced to less than $\pm 0.6\%$, approximately a third compared to normal firing order for the V8 engine. For this reason a parallel turbocharged V8 engine should

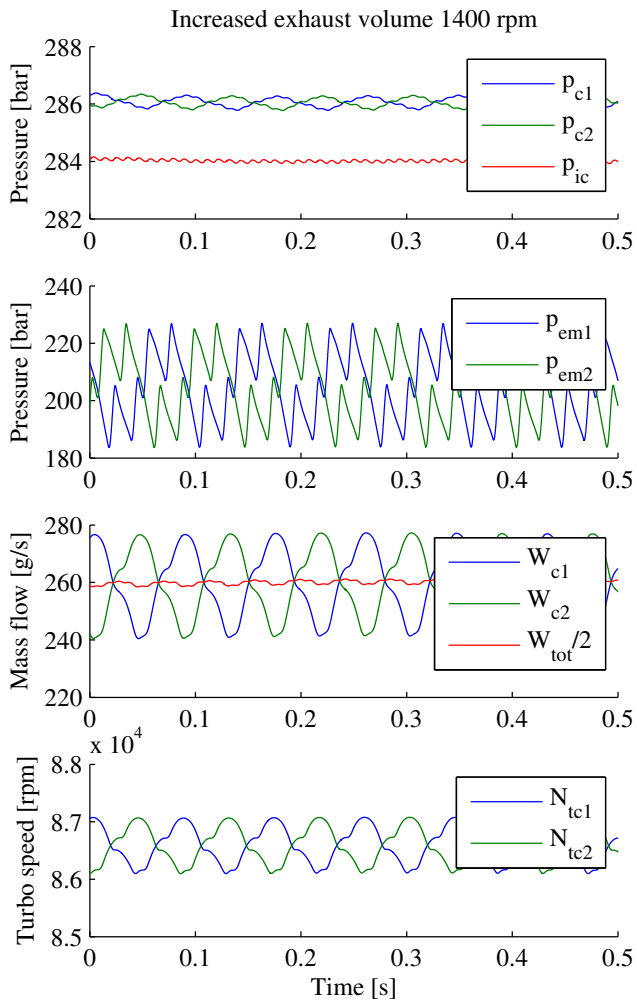


Figure 5. Simulation in a steady state operating point at 1400 rpm with increased exhaust manifold volume. This effectively reduces the pressure pulsation at the turbine inlet which reduce turbine speed and instantaneous mass flow oscillation. However it also reduces the available energy to the turbines which is not desirable.

be more sensitive to surge compared to a V6, when running low speed high torque operating points, where the compressor typically operates close to the surge line.

3.4 Impact on co-surge sensitivity

The cyclic variations in compressor speed results in large variations in compressor operating point. This is a consequence of the very flat characteristic of the speed lines immediately to the right of the surge line in the compressor map, see Fig. 2. Fig. 7 zooms in the compressor map around cyclic variations for the simulation in Fig. 4, which is shown by the blue line. The thin black dashed lines are compressor speed lines only 1000 rpm apart (85.5 krpm to 88.5 krpm). As evident, a very small change in compressor speed moves the operation point far in the mass flow direction for the compressor map. The green line show the corresponding variation for the simulation with altered ignition order from Fig. 6. The red line correspond a simulation with short-circuited exhaust manifolds - see Section 3.5.

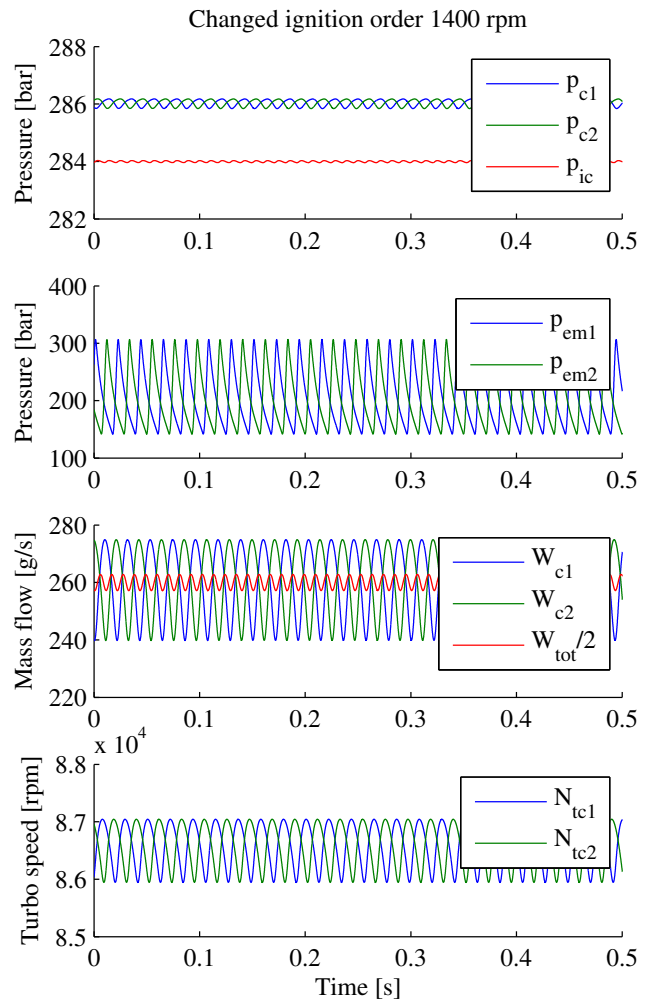


Figure 6. Simulation in a steady state operating point at 1400 rpm, with changed firing order so that each cylinder bank fires one cylinder every 180°. For this hypothetical situation the turbo speed oscillation is only about a third compared to the real firing order, and the same is true for the mass flow oscillation.

To quantify the difference in surge sensitivity, ramps in engine speed with fixed boost pressure reference was performed. The starting point was the fixed operating point in Fig. 4-6, at 1400 rpm. Then the engine speed was lowered until the model entered co-surge. For the base model this occurred around 1250 rpm, and for the changed ignition order around 1000 rpm, which is a significant difference. With increased exhaust manifold volume or double turbocharger inertia the system also enters surge slightly above 1000 rpm, but for that case with increased volume the available energy to the turbines were insufficient to keep the boost pressure at the same level.

3.5 Short-circuited exhaust manifolds

Since the large part of the turbo speed difference originates from the fact that the exhaust pulses alternately powers one of the turbines, one possible way to reduce this would be to short-circuit the exhaust manifolds. This transfers some of the exhaust energy from one bank to the other but has the downside that part of the exhaust pulse energy is lost. As an

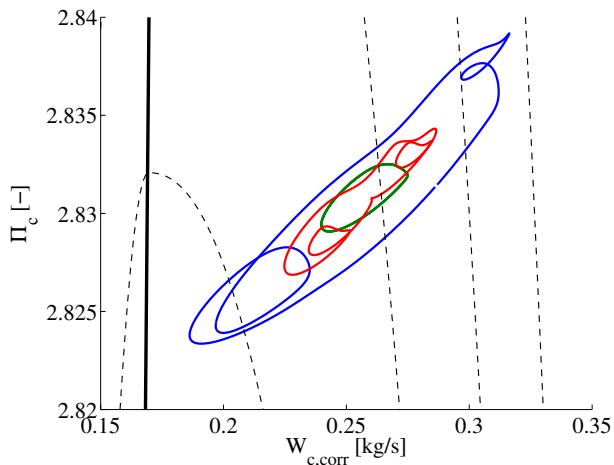


Figure 7. Compressor map zoomed in around cyclic operation for the simulation shown in Fig. 4. The blue and green lines corresponds to the compressor operation for simulations in Fig. 4 and Fig. 6 respectively. The red line shows the compressor operation with a short-circuit pipe between the exhaust manifolds.

example, with a 1 m long and 3 cm wide short-circuit pipe, modeled with two compressible restrictions and a control volume, the resulting compressor operation is shown by the red line Fig. 7. Doing the same engine speed ramp as in the previous section, the system enters surge around 1150 rpm, 100 rpm lower than the base configuration. Increasing the size of the pipe would trade available energy for more balanced turbo speeds. Adding controllable valves to the pipe could open for the possibility of utilizing the full pulse energy in operating points with more margin to the compressor surge line, and reducing the pulse energy in favor of more balanced operation closer to the surge limit.

4 Conclusions

The simulations study shows that the main source of cyclic variations in mass flow balance in parallel turbocharged engines is due to oscillations in turbo speed. This is mainly a result of exhaust pulsations, which has additional consequence for the V8 engine due to its firing order. Since two cylinders will fire in sequence once each engine cycle on each bank, the turbo speed oscillation will be larger compared to for example a similar sized four cylinder engine with a single turbocharger or a parallel turbocharged V6 engine where the cylinder on each bank fires with equal angle between them. For this reason parallel turbocharged V8 engines should be more sensitive to surge and require larger margin to the surge line compared to parallel turbocharged V6 engines. A way to reduce the cyclic variation is to short-circuit the exhaust manifolds. This reduces the surge sensitivity, but the trade off is a reduction in the available energy in the exhaust pulses.

References

Franz G. Chmela and Gerard C. Orthaber. Rate of Heat Release Prediction for Direct Injection Diesel Engines Based on Purely

Mixing Controlled Combustion. In *SAE World Congr.*, Techn. Paper 1999-01-0186, March 1999.

K.-D. Emmenthal, G. Hagermann, and W.-H. Hucho. Turbocharging small displacement spark ignited engines for improved fuel economy. In *SAE World Congr.*, Techn. Paper 790311, February 1979.

Lars Eriksson. Modeling and Control of Turbocharged SI and DI Engines. *Oil & Gas Science and Technology - Rev. IFP*, 62(4):523–538, 2007.

J. Galindo, H. Climent, C. Guardiola, and J. Domenech. Strategies for improving the mode transition in a sequential parallel turbocharged automotive diesel engine. *Int. J. of Automotive Technology*, 10(2):141–149, 2009.

E.M. Greitzer. Surge and rotating stall in axial flow compressors—Part I: Theoretical compression system model. *J. of Engineering for Power*, 98(2):190–198, April 1976.

E.M. Greitzer. The Stability of Pumping Systems. *J. of Fluids Engineering*, 103(1):193–242, June 1981.

L. Guzzella, U. Wenger, and R. Martin. IC-Engine Downsizing and Pressure-Wave Supercharging for Fuel Economy. *SAE World Congr.*, March 2000.

Lino Guzzella and Alois Amstutz. Control of Diesel Engines. *Control Systems*, 18(5):53–71, 1998.

K.E. Hansen, P. Jørgensen, and P.S. Larsen. Experimental and Theoretical Study of Surge in a Small Centrifugal Compressor. *J. of Fluids Engineering*, 103(3):391–395, 1981.

Elbert Hendricks. The Analysis of Mean Value Engine Models. In *SAE World Congr.*, Techn. Paper 890563, February 1989.

Elbert Hendricks and Spencer C. Sorenson. Mean value modelling of spark ignition engines. *SAE Trans. J. of Engines*, 99(3):1359–1373, 1990.

John B. Heywood. *Internal Combustion Engine Fundamentals*. McGraw-Hill series in mechanical engineering. McGraw-Hill, 1988. ISBN 0-07-100499-8.

J.-P. Jensen, A. F. Kristensen, S. C. Sorenson, N. Houbak, and E. Hendricks. Mean Value Modeling of a Small Turbocharged Diesel Engine. In *SAE World Congr.*, Techn. Paper 910070, February 1991.

Oskar Leufvén and Lars Eriksson. A Surge and Choke Capable Compressor Flow Model - Validation and Extrapolation Capability. *Control Engineering Practice*, 21(12):1871–1883, 2013.

Dominique Petitjean, Luciano Bernardini, Chris Middlemass, S. M. Shahed, and Ronald G. Hurley. Advanced Gasoline Engine Turbocharging Technology for Fuel Economy Improvements. In *SAE World Congr.*, Techn. Paper 2004-01-0988, March 2004.

Andreas Thomasson and Lars Eriksson. Modeling and Control of Co-Surge in Bi-Turbo Engines. In *Proc. of the IFAC World Congr.*, Milano, Italy, 2011.

Andreas Thomasson and Lars Eriksson. Co-Surge in Bi-Turbo Engines - Measurements, Analysis and Control. *Control Engineering Practice*, 32:113–122, November 2014.

N. Watson and M.S. Janota. *Turbocharging the Internal Combustion Engine*. The Macmillan Press Ltd, 1982. ISBN 0-333-24290-4.

Fredrik Westin. *Simulation of turbocharged SI-engines - with focus on the turbine*. PhD thesis, Royal Institute of Technology, May 2005.

G. Woschni. A Universally Applicable Equation for the Instantaneous Heat Transfer Coefficient in the Internal Combustion Engine. In *SAE World Congr.*, Techn. Paper 670931, February 1967.